High-Performance HTLcs-Derived CuZnAl Catalysts for Hydrogen Production via Methanol Steam Reforming

Ying Tang, Ye Liu, Ping Zhu, Qingsong Xue, Li Chen, and Yong Lu
Shanghai Key Laboratory of Green Chemistry and Chemical Processes, Dept. of Chemistry, East China Normal University, Shanghai 200062, China

DOI 10.1002/aic.11753
Published online March 25, 2009 in Wiley InterScience (www.interscience.wiley.com).

A series of CuZnAl oxide-composite catalysts were prepared via *decomposition of CuZnAl hydrotalcite-like compounds (HTLcs). The catalysts derived from CuZnAl HTLcs (Cu: 37%, Zn: 15%, Al: 48% mol; using metal nitrate or acetate precursors) at 600°C provided excellent activity and stability for the methanol steam reforming. CuZnAl HTLcs were almost decomposed completely at 600°C to form highly dispersed CuO with large specific surface area while forming $CuAl_2O_4$ spinel that played a key role in separating and stabilizing the nano-sized Cu and ZnO during the reaction. The CuZnAl catalyst prepared from metal acetates could highly convert H_2O/MeOH (1.3/1, mol/mol) mixture into hydrogen with only ~0.05% CO at 250°C or ~0.005% at 210°C. It is evidenced that the former afforded stronger Cu-ZnO interaction, which might be the intrinsic reason for the significant promotion of catalyst selectivity.*
 AIChE J, 55: 1217–1228, 2009
Keywords: catalysis, hydrotalcite, methanol steam reforming, hydrogen, fuel cells

Introduction

The depletion of fossil fuel reserves along with the increasingly stringent new air-quality standards make H_2-fed polymeric electrolyte membrane fuel cell (PEMFC) an attractive alternative to internal combustion engines in expandable applications, such as passenger propulsion, distributed and auxiliary power systems. Until widespread hydrogen refueling infrastructure exists, however, on-board hydrogen production technology starting from a suitable liquid source appears to be a practical option in a medium-short perspective. One of the most prominent liquid fuels for the use with on-board fuel processor to produce hydrogen is methanol. This is due to the following superior advantages including: low reaction temperature (~250°C), simple molecule with high H/C molar ratio, one-step reaction to H_2-rich reformates with low-level CO concentration, lack of sulfur/nitrogen compounds, minor effort on changing the fueling station (from gasoline or diesel), and attractive possibility to be produced from biomass.[1,2] Among the reformation technologies of methanol, methanol steam reforming (MSR) is considered to be the most favorable process of hydrogen production process because of the ability to produce gas with high hydrogen concentration (~75%). Nevertheless, a heating source such as catalytic burner is needed for the reaction energy supply.

Extensively studied MSR catalysts are mostly based on copper nano-particles deposited or incorporated into various supports such as ZnO,[3] $ZnO\text{-}Al_2O_3$,[4–7] $Cr_2O_3\text{-}Al_2O_3$,[8] $CeO_2\text{-}(ZnO)\text{-}Al_2O_3$,[9] and $ZrO_2\text{-}Al_2O_3$.[10] Eventually, Cu-ZnO (Al_2O_3) catalysts are promising and provide quite good activity/selectivity, but suffer from poor long-term stability that stems from the sintering of surface-active copper particles during the reaction. Recently, hydrotalcite-like compounds (HTLcs), important lamellar solids, are attracting growing interest in catalysis because of a homogeneous distribution of cation in the structure and therefore the formation of

Additional Supporting Information may be found in the online version of this article.

Correspondence concerning this article should be addressed to Y. Lu at ylu@chem.ecnu.edu.cn

homogeneous stable oxide composites by thermal decomposition.[11] CuZnAl catalysts derived from HTLcs, which are obtained by coprecipitating metal chlorates with a modified urea method, have been reported to be active and selective for oxidative steam reforming of methanol (OSRM) and characterized deeply in items of acid–base and redox properties of the catalysts.[12,13]

Despite these advances, studies on the structure-performance (activity, selectivity and stability) relationships of the HTLcs-derived CuZnAl catalysts for the reforming of methanol are not sufficient, because we should always bear in mind that the microstructure of the active copper phase of the CuO/ZnO catalysts are strongly dependent on the preparation parameters of coprecipitation[14–19] that was found to be superior to the other methods such as impregnation, high-energy milling and hydrothermal synthesis.[20] For example, regarding the hydrogen production from methanol reforming, CuO/ZnO (Al_2O_3) catalysts that are prepared by either industrial precipitation method or thermal decomposition of HTLcs are all reported to be calcined or decomposed mostly at a single temperature point around 400°C.[14–19,21,22] However, the calcination temperature is indeed a key catalyst preparation parameter that strongly affects the catalytically relevant properties such as metal dispersion, phase structure and metal-support interaction.[23,24] It is thus conceivable to develop high-performance MSR CuZnAl catalysts from HTLcs compounds by carefully tuning the decomposition temperature and selecting the metal precursors for HTLcs synthesis.

In this work, a series of CuZnAl HTLcs were synthesized *via* Na_2CO_3/NaOH coprecipitation/crystallization method using nitrate, acetate, sulfate and chloride of copper and zinc as precursors. CuZnAl oxide-composite catalysts were then prepared by thermal decomposition of as-synthesized CuZnAl HTLcs and were examined for their use in the MSR for hydrogen production. Effects of decomposition temperature and metal salt precursor were investigated on the catalyst performance. We show that a mixture of H_2O/MeOH (1.3/1, mol/mol) can be highly converted into hydrogen just with a CO concentration as low as $\sim$ 0.05% (500 ppm) at 250°C or $\sim$0.005% (50 ppm) at 210°C over a HTLc-derived CuZnAl catalyst. To reveal the real reason for the significant improvement of catalyst performance (especially on selectivity to CO and stability), the catalytically relevant physiochemical properties of the HTLcs-derived CuZnAl oxides in items of copper dispersion/surface area of copper, specific surface area, bulk structures, Cu-ZnO interaction and basicity were studied by N_2O-titration, N_2-BET, X-ray diffraction (XRD), hydrogen temperature programmed reduction (H_2-TPR) combined with CO_2 constant temperature oxidation, and CO_2 temperature programmed desorption (CO_2-TPD).

Experimental

Catalyst preparation

A series of CuZnAl HTLcs were synthesized *via* traditional Na_2CO_3/NaOH coprecipitation method extensively described in detail elsewhere,[25] using A.R. grade nitrates, acetates, sulfates and chlorides of copper and zinc as precursors. Note that aluminum nitrate was always used as aluminum source.

CuZnAl oxide-composite catalysts were then obtained by thermal decomposition of the corresponding HTLcs in air. The decomposition procedure was programmed from room temperature to set point at a heating ramp of 1°C/min with a hold time of 3 h at the final temperature. Catalyst products were designated CuZnAl, -A, -Cl, or -S followed by a number that represented the decomposition temperature, wherein the characters of N, A, Cl and S indicated that the corresponding HTLcs were synthesized using nitrates, acetates, chlorides and sulfates, respectively. Catalyst particles of 100–250 μm were collected for the reaction use.

Characterizations

Decomposition behavior analyses of the HTLcs were performed on a Mettler TG-SDTA-851 analyzer with sample loading of approximately 20 mg. The temperature was raised from 25 to 800°C at heating rate of 5°C/min in a flow of air (30 mL/min). Determination of phase structure and specific surface area of samples was performed *via* XRD and N_2-BET method extensively described in detail elsewhere.[26]

Catalyst basicity determination by the CO_2-TPD and CuO reducibility measurement by H_2-TPR were carried out on a Quantachrome ChemBET 3000 chemisorption apparatus fitted with a TCD. For H_2-TPR experiments, the temperature of sample was ramped at 10°C/min in 5% H_2/Ar flow of 40 mL/min. For CO_2-TPD experiments, adsorption was conducted by using 5% CO_2/He flow of 30 mL/min to pass through the sample bed at room temperature for 1 h, and the desorption was carried out in He flow.

Surface area of copper per gram catalyst and copper dispersion were estimated by the N_2O titration method[27] on a Quantachrome ChemBET 3000 chemisorption instrument, in according to $2Cu_{(surface)} + N_2O \rightarrow Cu_2O_{(surface)} + N_2$. Firstly, the sample of $\sim$10 mg (fresh and used) underwent a H_2-TPR process in 5% H_2/Ar mixture from 25 to 450°C for prereduction. Then, N_2O oxidation was carried out by feeding 5% N_2O/Ar to the sample bed at a flow rate of 80 mL/min at 60°C for 1 h, followed by Ar purging and cooling the sample bed down to room temperature. Finally, H_2-TPR was performed again with a gas mixture of 5% H_2/Ar to 450°C. Therefore, the surface area of copper per gram catalyst could be obtained according to the H_2 consumption ($H_2 + Cu_2O_{(surface)} \rightarrow Cu_{(surface)} + H_2O$) and the copper atom area of 6.8×10^{-20} m^2. Moreover, copper dispersion (D_{Cu}) was defined as below.

$$D_{Cu} = \frac{2 \times (\text{H}_2 \text{ consumption for } \text{Cu}_2\text{O reduction in 2nd } \text{H}_2-\text{TPR})}{\text{H}_2 \text{ consumption for CuO reduction in 1st } \text{H}_2-\text{TPR}} \times 100\%$$

Redox properties of the HTLcs-derived CuZnAl catalysts were investigated by reduction-oxidation-reduction cycle technique. This cycle consisted of three consecutive steps: (i) a standard H_2-TPR run of a fresh catalyst as described above; (ii) an oxidation step by CO_2 at 300°C for 1 h using 5 vol % CO_2/He (40 mL/min); (iii) a second H_2-TPR run.

After the CO_2 oxidation [step (ii)], the residual CO_2 was rapidly removed from the reactor by Ar purging (80 mL/min) and the sample was quickly cooled down to room temperature in Ar flow before starting the second TPR run.

FTIR spectra of both HTLcs and HTLcs-derived catalysts were recorded on a Nicolet Nuxes 670 spectrometer. Dosage of the powder mixture for disk preparation and the weight ratio of sample to KBr in the mixture were always kept constant.

Morphology and elemental mapping measurements for HTLcs-derived catalysts were performed on a field emission scanning electronic microscopy (FE-SEM, Hitachi S-4800) equipped with an energy despersive X-ray analyses (EDX) unit (Oxford, UK).

Reactivity test

Catalytic performance was conducted at atmospheric pressure in a continuous flow fixed-bed reactor consisting of a stainless-steel tube (12 mm i.d. by 700 mm long) placed in an electric furnace with a constant temperature region as long as 50 mm. Here catalyst of 1.5 g was loaded and directly exposed to reactant stream without any pretreatment. A H_2O/CH_3OH (1.3/1, mol/mol) mixture was fed continuously at a rate of 29 μL/min using a high-performance liquid chromatography (HPLC) pump, in parallel with pure N_2 (15 mL/min, as internal standard gas) feeding using a calibrated mass flow controller, into the reactor heated to the desired reaction temperature. Effluent from the reactor was cooled using ice-water bath to liquefy the condensable vapors. A HP 6850 gas chromatograph (GC) equipped with a TCD and a 30-m AT-plot capillary column was employed to analyze H_2, N_2, CO, CO_2, and C1–C3 hydrocarbons in the effluent, using He carrier and the column temperature programmed from 40 to 160°C at a ramp of 30°C/min with a hold time of 3 min at each of the initial and final temperatures. When CO product was lower than 500 ppm, another GC equipped with TCD and a 5A molecular sieve packed column was used for CO detection, which permitted big sample injection. Conversion and product composition were calculated by the N_2 internal standard method that is outlined as below,

$$F_{st} = F_{total}^{outlet} \times Y_{st}^{outlet} = F_{total}^{inlet} \times Y_{st}^{inlet}$$

where Y_{st}^{inlet} and Y_{st}^{outlet} denote concentration of the internal standard gas in the effluent gas (dry). Whereas the total flow rate changed significantly between the reactor inlet (F_{total}^{inlet}) and the outlet (F_{total}^{outlet}), the flow rate of the inert internal standard gas (F_{st}) is kept constant.

Therefore, formation rate of i product (F_i) can be calculated as

$$F_i = F_{total}^{outlet} \times Y_i^{outlet} = \frac{F_{st} \times Y_i^{outlet}}{Y_{st}^{outlet}}$$

Methanol conversion (C_{MeOH}) and concentration of i product in dry reformate (X_i, not including the internal standard gas) can be calculated as

$$C_{MeOH} = \frac{\sum F_i}{F_{MeOH,gas}} = \frac{F_{CO}^{outlet} + F_{CO_2}^{outlet} + F_{CH_4}^{outlet}}{F_{MeOH,gas}} \times 100\%$$

$$X_i = \frac{Y_i^{outlet}}{\sum Y_i^{outlet}} = \frac{Y_i^{outlet}}{Y_{CO}^{outlet} + Y_{CO_2}^{outlet} + Y_{CH_4}^{outlet} + Y_{H_2}^{outlet}} \times 100\%$$

Furthermore, catalyst activity was defined as the amount of methanol converted over per gram catalyst within per unit reaction time. Herein methanol conversion (C_{MeOH}) was able to be directly used to indicate the catalyst activity as the tests were all performed over 1.5 g catalysts with WHSV of 2.5 h^{-1}. Concentration of i product in dry reformate (X_i) divided by ΣX_i (i = CO, CO_2, CH_4) was defined as the carbon-containing product selectivity; clearly, the lower is the X_i, the lower is the selectivity to i product. The stability of the catalyst was defined as the ability of the catalyst for methanol conversion maintenance with prolonged time on stream. Note that turnover frequency (TOF), normalized methanol conversion by the number of surface Cu atoms per gram catalyst, were calculated and used to denote the intrinsic activity of the catalysts.

Results

XRD and TG/DTG analyses of HTLcs

Figure 1 shows the XRD patterns of the HTLcs with a Cu/Zn/Al molar ratio of 37/15/48 synthesized using nitrate, acetate, sulfate and chloride of copper and zinc as precursors. Clearly, the hydroxyl carbonates containing hydrotalcite-like layered double hydroxide could be obtained as primary phase in all cases but the crystallinity was decreased in following order: sulfate < chloride ≪ nitrate ~ acetate. Previous literature[28] reported that partial substitute of Cl^- or SO_4^{2-} for CO_3^{2-} of interlayer causes deformation of the

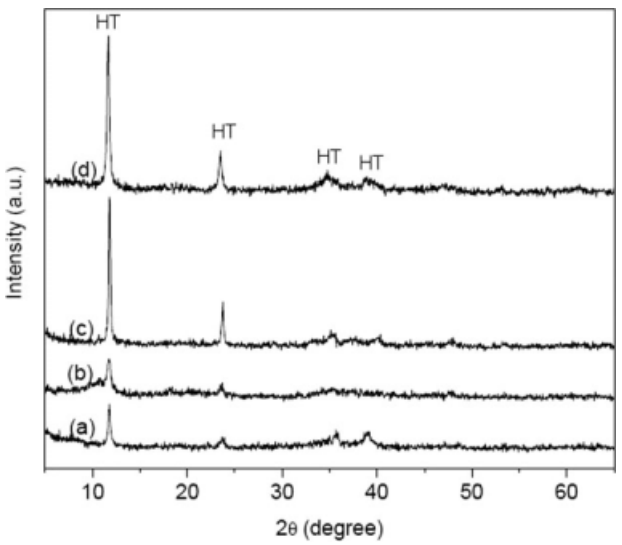

Figure 1. XRD patterns of CuZnAl HTLcs synthesized using aluminum nitrate and various copper/zinc sources of (a) chlorides, (b) sulfates, (c) acetates, and (d) nitrates.

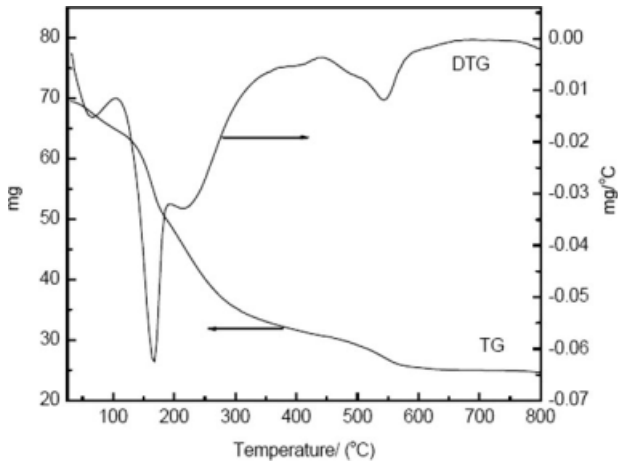

Figure 2. TG-DTG curves of CuZnAl HTLcs synthesized using metal nitrate precursors.

double-layer structure and octahedral metal hydroxide thereby lowering the crystallinity of HTLcs.

Figure 2 shows the thermogravimetric (TG) and corresponding derivative TG (DTG) curves of the HTLcs synthesized from nitrates as a function of temperature. It is clear that the TG/DTG curves showed typical features of the thermal decomposition of CuZnAl HTLcs,[29,30] which experienced decomposition through four steps upon heating in a flow of air. The weight loss below 100°C is ascribed to physically adsorbed water, and the sharply weight loss around 170°C is associated with the removal of condensation (interlayer) water in the HTLcs structure.[18,29,30] The third process, which is displayed as a broad peak in the range 200–400°C on the DTG curve, is ascribed to dehydroxylation and simultaneous decarbonation. These three weight-loss processes commonly involve in the thermal decomposition of hydrotalcite-like materials. However, unlike the HTLcs built up by Mg and Al, the thermal evolution process of Cu-containing HTLcs underwent the formation of transitional $(Cu,Zn)Al_xO_y(CO_3)_z$ compound,[24] which would be decomposed to form oxide composites at above 550°C as indicated by the broad peak in the range 450–600°C on the DTG curve. Similar thermal evolution process was obtained for the HTLcs synthesized using acetates (not shown), while the TG/DTG analyses did not proceed on the HTLcs synthesized using chlorides and sulfates because of their poor crystalinity.

Effect of decomposition temperature of HTLcs on catalytic reactivity

A series of catalysts were derived from CuZnAl HTLcs with Cu/Zn/Al (nitrate precursors) molar ratio of 37/15/48 through thermal decomposition at various decomposition temperatures, and were examined in the MSR process with the results as shown in Table 1. As we can see, all HTLcs-derived catalysts afforded good initial activity with methanol conversions of ca. 97–98% (*i.e.*, conversions after 1 h run). With reaction running to 10 h, the catalysts except the one decomposed at 600°C experienced obvious reduction of methanol conversions, and then the conversions almost remained without obvious change in the other 15 h test. Unlike the methanol conversion, the dry gas product composite almost remained constant with the increase in decomposition temperature of the HTLcs-derived catalysts: H_2: 75%, CO_2: 24.8%, CO: 0.2% mol; trace CH_4.

Actually, when the catalysts of CuZnAl-N-600, -700 and -800 (decomposed at 600, 700 and 800°C, respectively) were pre-reduced with H_2 at 300°C for 3 h and examined their use with the MSR under compatible reaction conditions as in Table 1, it was found that these three catalysts afforded methanol conversion values quite close to the numbers after 10 h test as listed in Table 1. Similar phenomena were also observed for CuZnAl-N-300, -400 and -500 catalysts. Thus, we think here that the conversions just after 10 h run can represent the true activity of these catalysts. In this initial reaction period, usually 5 h or longer for our catalysts, *in situ* reduction of CuO particles of the catalysts occurred likely to form Cu^0-Cu^+ twin sites, because Cu^0-Cu^+ twin is generally accepted to be the dominant structure in the real processes of the MSR and its reverse reaction.[31,32] In addition, our HTLcs-derived catalysts can be used directly with omitting the prereduction treatment. This is an important reformer consideration for application in portable or mobile fuel cell power systems, because the reformer can operate frequently between startup and shutoff (exposure of catalyst to air is possible).

Additionally, reaction test of the CuZnAl-N-600 catalyst was expanded to 100 h and the methanol conversion always remained >96% in entire test. This indicated that this catalyst showed excellent activity and stability, possibly because of its special structure that is one main objective in our present work.

From the foregoing reaction test, it can be postulated that close relationship between the catalyst performance (activity

Table 1. Effect of Decomposition Temperature for the HTLcs-Derived CuZnAl-N Catalysts on their Reactivity in the MSR Reaction*

	Methanol Conversion in Different Time Period (mol %)					
Decomposition Temperature (°C)	1 h	5 h	10 h	15 h	20 h	25 h
300	97.3	83.7	77.8	78.2	79.1	81.2
400	96.8	79.6	83.9	84.7	78.7	80.0
500	98.0	90.9	82.9	83.4	84.2	83.3
600	98.5	100	96.9	100	98.9	99.0
700	96.9	94.0	88.3	85.6	85.0	84.9
800	97.3	81.1	77.9	75.2	73.2	75.9

Reaction conditions: H_2O/CH_3OH molar ratio = 1.3:1, total WHSV = 2.5 h^{-1}, P = 0.1 MPa, T = 250°C.
*Same gaseous product composition (dry base) was obtained if ignored the random errors: H_2, 75.0 mol %; CO_2, 24.8 mol %; CO, 0.2 mol % (2000 ppm); CH_4, trace.

Table 2. Effect of Decomposition Temperature for the HTLcs-Derived CuZnAl-N Catalysts on their Physicochemical Properties

Decomposition Temperature (°C)	S_{BET} (m^2/g)	S_{Cu} (m^2/g)	D_{Cu} (%)	TOF* (h^{-1})
300	100	10.4	8.7	140.6
400	104	17.6	9.2	82.7
500	97	20.9	12.6	74.5
600	102	39.6	23.7	46.6
700	59	21.0	11.2	74.8
800	37	18.8	10.8	72.0

*TOF: Turnover frequency to methanol, deduced from the methanol conversion at 25 h as in Table 1.

and stability) and catalyst structure was strongly influenced by the decomposition temperature. It is believed that carefully characterizing these HTLcs-derived catalysts would give us clear answer to this speculation.

Effect of decomposition temperature of HTLcs on copper dispersion and specific surface area

Actually, dramatic effects of decomposition temperature on the catalytically relevant properties can be observed, first, from the surface area of copper, copper dispersion and specific surface area as listed in Table 2. It is clear from Table 2 that the specific surface areas remained almost constant ($\sim$100 m^2/g) with the increase in decomposition temperature up to 600°C and then decreased greatly with the further increase in the temperature to and above 700°C due to severe sintering. The decomposition of the HTLcs at 600°C endued the resulting catalyst with the largest surface area of copper and the highest copper dispersion. This is correlated well with the trend of methanol conversion against the catalyst decomposition temperature as shown in Table 1.

By combining the above information with the decomposition evolution of CuZnAl HTLcs as shown in Figure 2, it was believed that the small surface area of copper and copper dispersion could be ascribed to the incomplete decomposition of HTLcs with formation of $(Cu,Zn)Al_xO_y(CO_3)_z$ compounds at or below 500°C. The $(Cu,Zn)Al_xO_y(CO_3)_z$ compounds just could be decomposed completely at 600°C thereby maximizing the surface area of copper and copper dispersion. The use of too higher decomposition temperatures (*e.g.*, 700°C or higher), however, would cause severe copper sintering and meanwhile facilitate $CuAl_2O_4$ spinel formation as suggested by the posterior characterization results. This undoubtedly resulted in significant reduction of the surface area of copper and in turn degraded the catalyst activity.

The turnover frequencies (TOFs) to methanol were also listed in Table 2. Clearly, TOFs showed a reverse trend against the surface area of copper. It should be noted, however, that the change of TOFs was not proportional to the change of the surface area of copper. For example, increase in the decomposition temperature from 300 to 600°C almost quadrupled the surface area of copper but made TOF value deceased to 46.1 (a third of that for decomposition at 300°C) (Table 1), indicating that Cu^0 likely cannot represent the real active site on the working catalyst surface. As generally accepted, Cu^0-Cu^+ twin is the dominant structure in the real processes of the MSR and its reverse reaction.[31,32] However, measurement of the concentration of Cu^0-Cu^+ twin and in turn TOFs estimation based on Cu^0-Cu^+ twin concentration is difficult.[33,34]

Effect of decomposition temperature of HTLcs on catalyst phase structure

Phase structure of the HTLcs-derived CuZnAl catalysts (using nitrate precursors) as determined by the XRD versus decomposition temperature is depicted in Figure 3. The catalysts almost afforded quite faint CuO XRD peaks until the decomposition temperature was increased to 500°C. With further increasing the decomposition temperature to 600°C or higher, the CuO XRD peaks became sharper and stronger, and meanwhile, a new phase of $CuAl_2O_4$ spinel started to be formed, which was identified by new peaks situated at (2θ) 31.3, 36.9, 44.9, 55.7, and 59.4°. It should be noticeable that the starting appearance of $CuAl_2O_4$ spinel phase at 600°C is corresponding to the complete decomposition of $(Cu,Zn)Al_xO_y(CO_3)_z$ compound as illustrated in Figure 2. Additionally, no any ZnO phase could be observed by XRD for all catalysts, suggesting that ZnO highly dispersed in the sample.

FTIR analyses for these HTLcs-derived CuZnAl catalysts were also performed with the results as depicted in Figure 4. The band at 830 cm^{-1} has been assigned to out-of-plane deformation vibration of CO_3^{2-}; the band at 1530 cm^{-1} has been assigned to CO vibration in interaction with OH group of the brucite-like layers, whereas the other band at 1380 cm^{-1} is assigned to the carbonate C=O vibration.[35] The bands at 725 and 795 cm^{-1} have been assigned to $CuAl_2O_4$ spinel vibration and the characteristic stretching vibrations of CuO appear around 494 and 600 cm^{-1}.[36] As we can see from Figure 4, a remarkable and surprising effect occurred at 600°C: clear characteristic stretching vibrations of CuO appeared at around 494 and 600 cm^{-1}; the carbonate

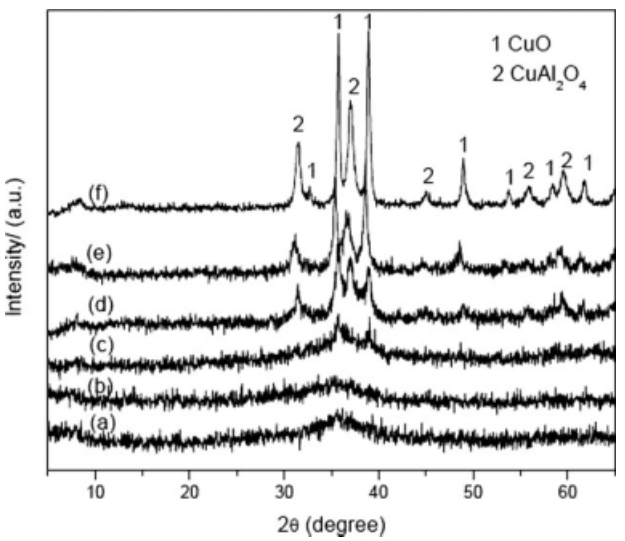

Figure 3. XRD patterns of the CuZnAl-N catalysts prepared by thermal decomposition of HTLcs synthesized using metal nitrate precursors at (a) 300°C, (b) 400°C, (c) 500°C, (d) 600°C, (e) 700°C, and (f) 800°C.

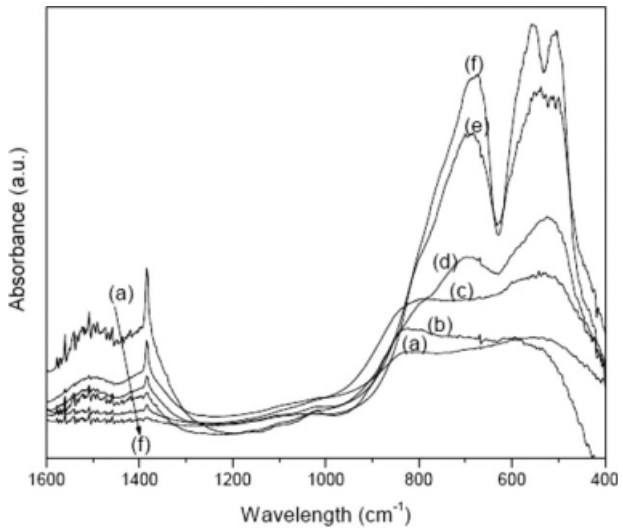

Figure 4. FTIR spectra of the CuZnAl-N catalysts prepared by thermal decomposition of HTLcs synthesized using metal nitrate precursors at (a) 300°C, (b) 400°C, (c) 500°C, (d) 600°C, (e) 700°C, and (f) 800°C.

band at 830 cm^{-1} decreased sharply while the other bands related to carbonate at 1530 and 1380 cm^{-1} became very weak. It should be noting that $CuAl_2O_4$ spinel phase vibrations[36] (at 725 and 795 cm^{-1}) started to appear at 600°C. A marked increase in the intensity of the bands related to CuO and $CuAl_2O_4$ spinel occurred upon increasing the temperature to 700–800°C. The above results showed excellent agreement with the results of XRD (Figure 3) and TG/DTG measurements (Figure 2).

Effect of decomposition temperature of HTLcs on catalyst reducibility by H_2-TPR

H_2-TPR profiles for the HTLcs-derived CuZnAl catalysts (using nitrate precursors) versus the decomposition temperature were summarized in Figure 5. For comparison, the H_2-TPR profile of pure CuO was also collected in the Figure 5, which showed a single peak with maximum at 340°C. It is clear that reduction behavior of the HTLcs-derived CuZnAl catalysts was strongly dependent on their decomposition temperatures.

The catalysts decomposed in temperature range 300–500°C all gave similar profiles consisting of an intense peak with a maximum at 370–380°C and a shoulder in the same temperature range as pure CuO. The main reduction peak was assigned to the reduction of Cu^{2+} ions incorporated in octahedral sites of the $(Cu,Zn)Al_xO_y(CO_3)_z$ compounds,[24] whereas the shoulder peak was contributed to the reduction of CuO products. This is in good agreement with the facts that $(Cu,Zn)Al_xO_y(CO_3)_z$ compounds would be produced when decomposing HTLcs at or below 500°C (Figure 2) and that the CuO phases just could be formed dominantly when decomposing HTLcs at or above 600°C (Figures 3 and 4).

Interesting H_2-TPR evolution was observed on the catalysts prepared by thermal decomposition of the HTLcs at 600, 700, and 800°C. A symmetric reduction peak appeared on the HTLcs-derived catalyst decomposed at 600°C, with the maximum at much lower temperature of 315°C compared with the other twos prepared by decomposing the HTLcs at 700 and 800°C. This agreed very well with the fact that the highest copper dispersion was obtained when decomposing at 600°C as listed in Table 2, because highly dispersed oxide particles (*i.e.*, small size) can reduce their reduction temperature. Moreover, the symmetric feature of this reduction peak might suggest that CuO was released uniformly with the narrow particle size distribution and the more homogeneous phase composition[37] might be obtained during the decomposition of HTLcs at 600°C.

The H_2-TPR profile consisting of a main peak at 330°C and a small shoulder at ~290°C was observed on the catalyst decomposed at 700°C. A symmetric reduction peak appeared again on the catalyst decomposed at 800°C, with the maximum peak temperature (340°C) equivalent to that of bulk CuO as illustrated in Figure 5a. The above results suggested that CuO phase was the primary product from HTLcs decomposition at or above 600°C, through the formation and subsequent decomposition of $(Cu,Zn)Al_xO_y(CO_3)_z$ compounds. Nevertheless, the primary CuO particles would aggregate to form larger CuO particles thereby leading to the increase of the reduction temperature as the decomposition temperature was increased at or above 700°C. Accordingly, the observation of the split reduction peaks for the sample decomposed at 700°C was ascribable to the incompletion of such aggregation process. By combining the above results with the information provided by XRD, FT-IR and TG/DTG, it is proposed additionally that, $CuAl_2O_4$ spinel was also the primary product from $(Cu,Zn)Al_xO_y(CO_3)_z$ decomposition at 600°C rather than the secondary product of solid reaction of CuO with Al_2O_3.

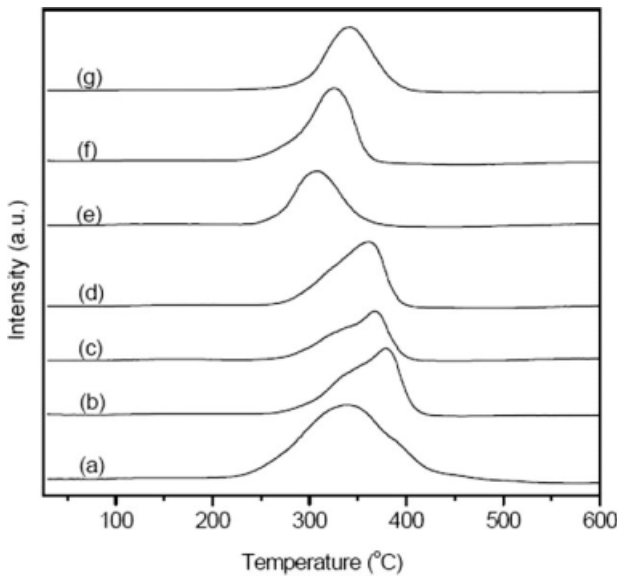

Figure 5. H_2-TPR profiles of (a) pure CuO and CuZnAl-N catalysts prepared by thermal decomposition of HTLcs synthesized using metal nitrate precursors at (b) 300°C, (c) 400°C, (d) 500°C, (e) 600°C, (f) 700°C, and (g) 800°C.

Table 3. Effect of Copper/Zinc Metal Salts for HTLcs Synthesis on the MSR Performance of their Derived CuZnAl Catalysts

Catalyst	Cu & Zn Precursor*	MeOH Conversion (mol %)	Dry Product Gas Composition (mol %)			
			H_2	CO_2	CO	CH_4
CuZnAl-N-600	Nitrates	99.0 (25 h)	75.0	24.8	0.20	trace
		97.5 (100 h)	75.3	24.6	0.16	trace
CuZnAl-A-600	Acetates	99.1 (25 h)	74.9	25.0	0.06	trace
		98.4 (100 h)	74.7	25.3	0.04	trace
CuZnAl-S-600	Sulfates	<5 (Initial)	74.3	25.7	0	trace
		3.2 (25 h)	71.4	28.6	0	trace
CuZnAl-C-600	Chlorides	7.9 (Initial)	76.1	23.5	0.36	trace
		7.8 (25 h)	75.0	24.6	0.43	trace

Reaction conditions: H_2O/CH_3OH molar ratio = 1.3:1, Total WHSV = 2.5 h^{-1}, P = 0.1 MPa, T = 250°C.
*$Al(NO_3)_3{\cdot}6H_2O$ was used as Al sources in all cases of HTLcs synthesis.

Effect of starting material for HTLcs synthesis on catalytic performance

Table 3 shows the catalytic performance of the CuZnAl catalysts derived from HTLcs synthesized from different metal precursors for the MSR process. Clearly, CuZnAl-A-600 that was prepared using metal acetates as precursors provided selectivity superior to the ones from nitrates, chloride and sulfates. For example, CuZnAl-A-600 afforded much lower CO concentration in the dry product gas compared with the CuZnAl-N-600 prepared from nitrates: 0.04–0.05% (400–500 ppm) vs. ~0.2% (2000 ppm) with >95% methanol conversion under compatible reaction conditions. Figure 6 shows the methanol conversion and the product composition over CuZnAl-A-600 in a long-term test. Likewise, this catalyst maintained its activity (>98%) with CO concentration of 0.03–0.05% (300–500 ppm) in the dry product gas for the entire 100 h test at 250°C (Figure 6A).

It should be noting that over CuZnAl-A-600 the CO concentration could be reduced further to ~0.005% (50 ppm) with near complete methanol conversion when decreasing the reaction temperature from 250 to 210°C along with WHSV from 2.5 to 0.5 h^{-1}, and these results remained over another 100-h test (Figure 6B). It is safe to say that one-step preparation of H_2, with the CO concentration as low as the requirement in PEMFC application, is possible *via* MSR process over the rationally designed CuZnAl catalysts.

In contrast, CuZnAl-S-600 and CuZnAl-C-600 that were derived from HTLcs synthesized using sulfates and chlorides of copper and zinc were inactive for the MSR reaction, affording methanol conversion less than 10%. Barton and Pour[38] reported that the presence of trace S and Cl (*e.g.*, 5 μg/g) in the feed stream can fast deactivate the MSR CuZnAl catalysts. They also suggested that the observation of the deactivation is due to the formation of volatile copper chloride compound or ZnS.[38] In our cases, the residual contents of S and Cl for CuZnAl-S-600 and CuZnAl-C-600 catalysts were determined to be 3.1 by ICP and 0.45 mg/g by ion chromatography, probably far beyond the endurable level for CuZnAl catalysts for the MSR reaction.

Effect of starting material for HTLcs synthesis on catalyst phase structure and reducibility

Phase composition of CuZnAl catalysts derived from HTLcs synthesized using various metal salts as determined by the XRD is depicted in Figure 7. The HTLcs synthesized using metal acetates offered a TG/DTG curve (not shown) same as that of the HTLcs synthesized using metal nitrates as indicated in Figure 2. Not surprisingly, the CuZnAl-A-600 catalyst provided a XRD pattern quite similar with the CuZnAl-N-600, consisting of CuO and $CuAl_2O_4$ spinel phases with comparable peak intensity (Figure 7). Likewise, the $CuAl_2O_4$ spinel can isolate and stabilize the Cu particles

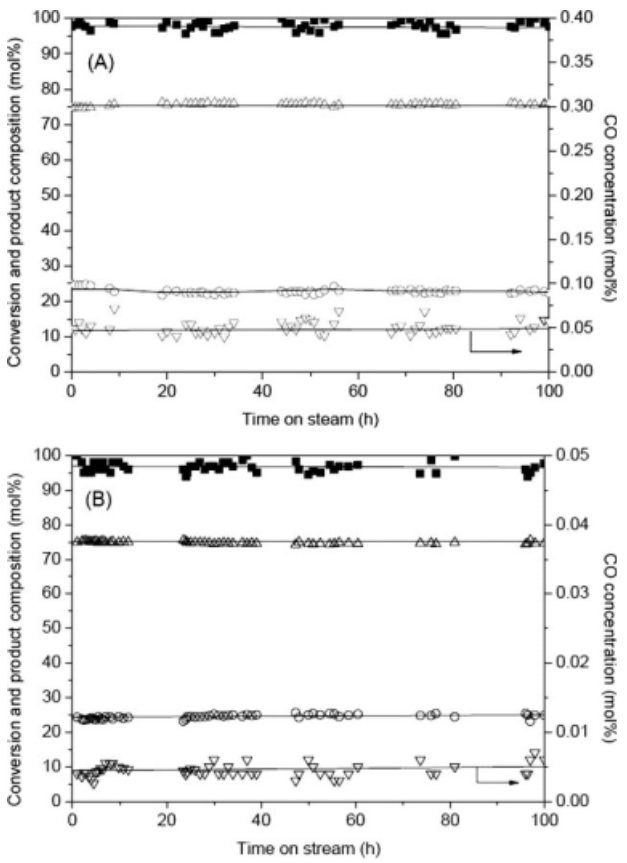

Figure 6. Longer-term test of MSR over the CuZnAl-A-600 catalyst under (A) 250°C and WHSV of 2.5 h^{-1} and (B) 210°C and WHSV of 0.5 h^{-1} after test A.

(Solid square) methanol conversion, (Open triangle) H_2 fraction, (Open circle) CO_2 fraction, (Open reverse triangle) CO fraction.

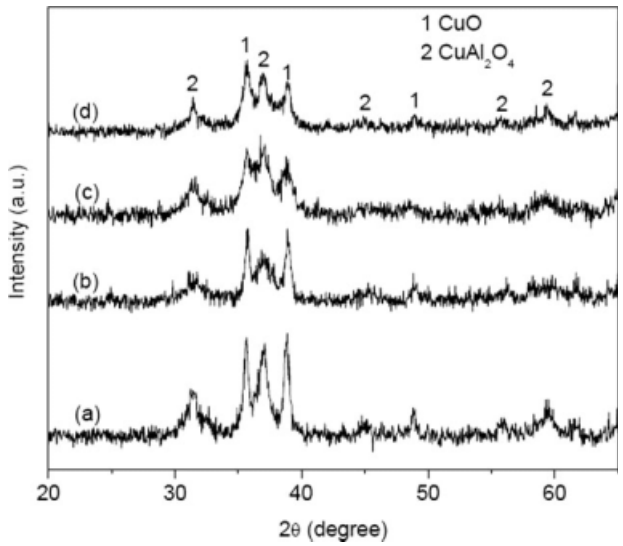

Figure 7. XRD patterns of the HTLcs-derived CuZnAl catalysts using a decomposition temperature of 600°C.

The HTLcs were synthesized using aluminum nitrate as aluminum source and various copper/zinc sources of (a) chlorides, (b) sulfates, (c) acetates, and (d) nitrates.

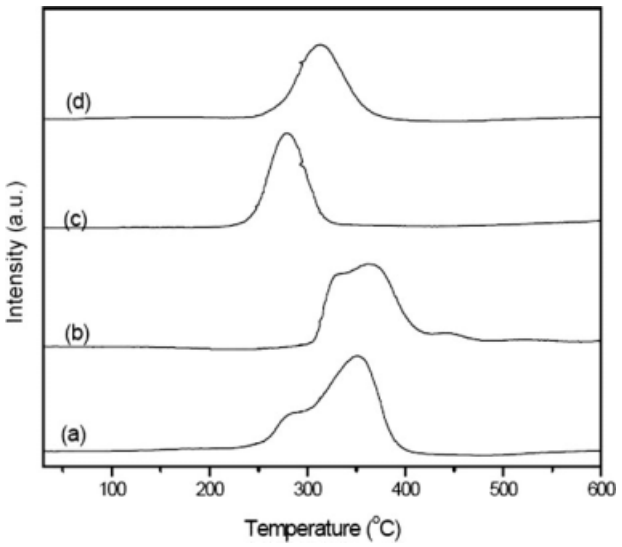

Figure 8. H_2-TPR profiles of the HTLcs-derived CuZnAl catalysts same as in Figure 7.

on the working catalyst surface thereby showing pleasing reaction stability (Figure 6).

Both CuO and $CuAl_2O_4$ spinel phases were also observed for CuZnAl-Cl-600 and CuZnAl-S-600 (Figure 7). Their CuO XRD peak became narrow and strong compared with CuZnAl-A-600 and CuZnAl-N-600. The above observations were ascribable to the poor crystallinity of as-synthesized HTLcs when using sulfates and chlorides of copper and zinc (Figure 1). As a result, the consequent agglomeration of CuO during the decomposition process was unavoidable, making copper dispersion quite low (Table 4). Larger size of the CuO particles except S and Cl poisoning might be another reason for their poor activity (Table 3). Nevertheless, the observations of the sharper and stronger CuO XRD peak for CuZnAl-C-600 and CuZnAl-S-600 seemed not proportional to the dramatic decrease in copper dispersion as listed in Table 4, compared with CuZnAl-N-600 and CuZnAl-A-600. The reason was not clear yet, probably due to the poisoning effect of S and Cl residues[38] that also strongly suppressed the oxidation of Cu with N_2O. In addition, Table 4 shows again that TOFs offered a reverse trend against the surface area of copper, which is consistent with the observation as indicated in the Table 2.

Table 4. Effect of Copper/Zinc Metal Salts for HTLcs Synthesis on the Physicochemical Properties of their Derived CuZnAl Catalysts

Catalyst	S_{BET} (m^2/g)	S_{Cu} (m^2/g)	D_{Cu} (%)	TOF* (h^{-1})
CuZnAl-N-600	102	39.6	27.4	46.6
CuZnAl-A-600	103	42.0	28.2	45.8
CuZnAl-S-600	70	3.1	5.5	4.1
CuZnAl-C-600	71	4.9	9.0	10.5

*Turnover frequency to methanol, deduced from the methanol conversion at 25 h as in Table 3.

Figure 8 shows the H_2-TPR profiles of the CuZnAl catalysts derived from HTLcs synthesized using various metal salts. Single symmetric peaks were observed for both CuZn Al-A-600 and CuZnAl-N-600 catalysts but multi-peak profiles for CuZnAl-S-600 and CuZnAl-Cl-600 catalysts. As explained clearly in the foregoing section, the symmetric feature of the H_2-TPR peak implied uniform CuO particle size and the more homogeneous phase composition (Figure 5). By contraries, according to the multi-peak features of H_2-TPR profiles for CuZnAl-S-600 and CuZnAl-Cl-600 catalysts, the particle size distribution and chemical properties of the CuO seemed not uniform. Interestingly, CuZnAl-A-600 catalyst offered a 35°C reduction of peak temperature compared with CuZnAl-N-600 catalyst. As indicated in the posterior section, this was ascribable to the difference in the interaction between CuO and ZnO, which was the essential reason for significant reduction of the CO concentration in the dry product gas.

Discussion

Role of $CuAl_2O_4$ spinel phase

To gain insight into the suppressive effect of the $CuAl_2O_4$ spinel phase on the aggregation of copper particles during reaction, which is significant risk factor affecting the catalyst durability, the CuZnAl-N-500, -600, and -700 catalysts after used for different time periods were analyzed by N_2O-titration. Their copper surface areas against the reaction time were summarized in Table 5. As we can see, the copper surface area decreased by >30% for CuZnAl-N-500 and ~5% for CuZnAl-N-600 along with increasing the reaction time from 5 to 10 h, and then remained without obvious change with further increasing the reaction time to 25 h for CuZnAl-N-600. The copper surface area also remained unchanged on CuZnAl-N-700 in this course, indicating that

Table 5. Surface Areas of Copper for the CuZnAl-N Catalysts after used in the MSR for Different Time Periods

Time on Stream (h)	S_{Cu}* (m^2 g^{-1})		
	CuZnAl-N-500†	CuZnAl-N-600†	CuZnAl-N-700†
0 (fresh)	20.9	39.6	21.0
15	14.0	37.5	20.9
25	13.9	37.2	20.5

*Determined by N_2O chemisorption.
†Used catalysts are same as those listed in Table 1.

the low conversion in Table 1 is assignable to small copper surface area (Table 5) rather than the copper sintering.

It is clear from Figure 3 that fresh CuZnAl-N-400 and −500 catalysts afforded faint XRD peaks of CuO compared with the fresh CuZnAl-N-600. However, after 25-h reaction both of CuZnAl-N-400 and -500 catalysts provided stronger XRD peaks of Cu than the CuZnAl-N-600 did (Figure 9), being consistent with the significant reduction of copper surface area (Table 5). This indicates that severe copper sintering occurred within 25-h run, which is the main cause of the low conversion of CuZnAl-N-300, -400, and -500 catalysts after 10 h on stream as shown in Table 1. Moreover, no visible increase of the XRD peak intensity of Cu occurred on the CuZnAl-N-600 catalyst even after 100-h reaction (Figure 9), being consistent with the observations of a little reduction of copper surface area within 25-h reaction (Table 5) and of its good activity maintenance within 100-h test (Table 3).

The above results were in good agreement with their reactivity behavior against the reaction time (Table 1). By combining the above results with the fact that the $CuAl_2O_4$ spinel phase was produced at or above 600°C, it is believed that, the $CuAl_2O_4$ spinel phase played a key role in isolating and stabilizing the copper particles on catalyst surface during the MSR reaction.

Cu-ZnO interaction and its correlation with the CO formation

Until now many investigations have been carried out with respect to the interaction between Cu and ZnO and the surface active sites of Cu-based catalysts for methanol synthesis.[29,39] However, the nature of the interaction is still controversial. For example, Klier[40] have ascribed the interaction to the Cu^+ in ZnO matrix, whereas Frost[41] contributes the interaction to the Schottky junction between the metal and the semiconducting oxide support. Regardless the type of the interaction, significant effect of this interaction on the catalytic intermediate, such as formate species, has been discussed by Neophytides et al.[42] and Yang et al.[36] in methanol synthesis. The same intermediates have also proven to be present in the MSR.[43,44] Likewise, the Cu-ZnO interaction likely plays a key role in tuning the catalytic intermediate formation in MSR, which in turn decisively promotes the catalyst selectivity. This point was emphatically discussed in the present work.

The present results demonstrated that Cu and Zn salts used for HTLcs synthesis have great influence on CO selectivity for the HTLcs-derived catalysts. As shown in Table 4, at equivalent methanol conversion (95–98%) the CO concentration in the dry product was 0.04–0.05% (400–500 ppm) at 250°C for the CuZnAl-A-600 catalyst prepared from acetates, just a fourth of that for the CuZnAl-N-600 catalyst prepared from nitrates. According to the definition of the product selectivity in Experimental section, for example, CO selectivity at 250°C was: ~0.2% for the CuZnAl-A-600 vs. ~0.8% for the CuZnAl-N-600. It is clear that the CO selectivity is well parallel to the CO concentration in the dry reformate, i.e., the lower CO concentration in the dry reformate, the lower the CO selectivity. It is noticeable that there has no correlation between the CO selectivity and the copper dispersion due to their close values as shown in Table 4.

Therefore, the scope of key factors that might affect the CO selectivity was firstly focused by briefly taking insight into the mechanism on the MSR. It seems widely accepted that methanol/H_2O was converted into CO_2 and H_2 through one-step pathway rather than methanol first decomposed to CO/H_2 and then the CO reacted with H_2O to form CO_2 and more H_2.[45–47] Among the studies of mechanistic aspect of the formation of CO as by-product in that one-step pathway, methyl formate has been regarded as a main intermediate confirmed by some researchers.[43,44]

The methyl formate would decompose to form carbon monoxide plus methanol and this process would be promoted if the catalyst basicity was enhanced.[48] Is it possible that the basicity of these two catalysts was different thereby leading to the difference in CO selectivity? To answer this question, the surface basic properties for both CuZnAl-N-600 and CuZnAl-A-600 catalysts were analyzed using CO_2-TPD. As shown in Figure 10, both catalysts provided similar CO_2-TPD profiles consisting of a main peak centered at 350°C and a shoulder peak at the low-temperature side, indicating that their basic strength and distribution was quite equivalent. Moreover, their surface basic sites per surface copper atom (*i.e.*, basic density) were also very close: 1.14×10^{-3} for CuZnAl-N-600 catalyst and 1.18×10^{-3} for CuZnAl-A-600 catalyst, respectively. Likewise, the difference in the CO

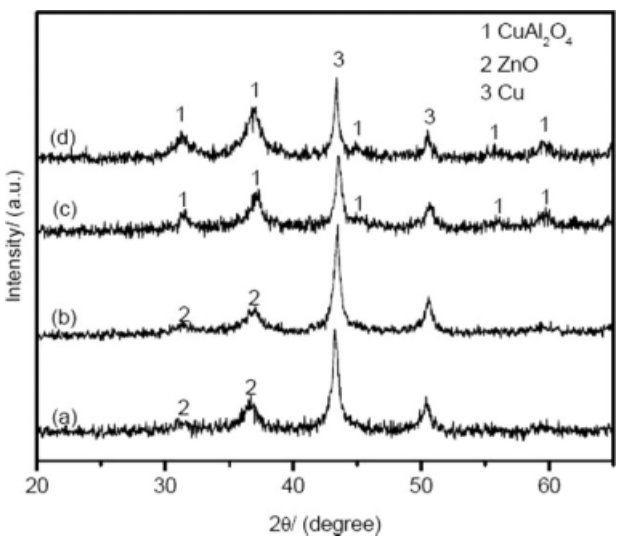

Figure 9. XRD patterns of (a) CuZnAl-N-400, (b) CuZnAl-N-500 and (c) CuZnAl-N-600 after reaction at 250°C for 25 h and (d) CuZnAl-N-600 after reaction at 250°C for 100 h.

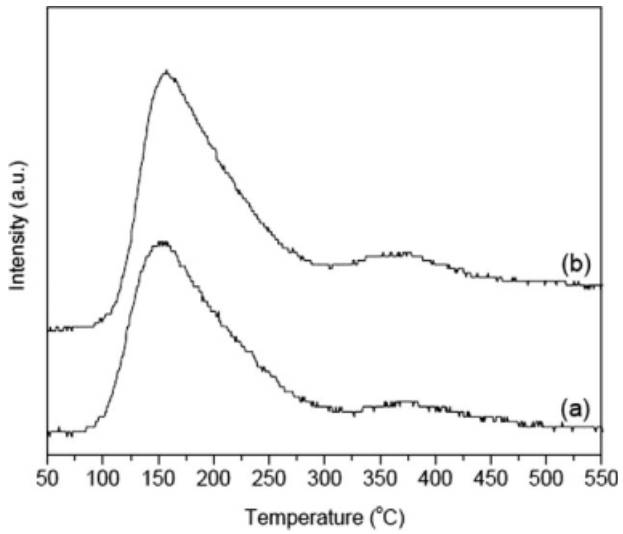

Figure 10. CO_2-TPD of (a) CuZnAl-N-600 and (b) CuZnAl-A-600 catalysts.

selectivity is not ascribable to the basic properties for these two catalysts.

However, H_2-TPR results showed that the reduction behavior was clearly different for these two catalysts (Figure 8). The reduction peak temperature was consistent with the CO concentration in the dry gas product for CuZnAl-A-600 and CuZnAl-N-600 catalysts: CO of 400–500 vs. 2000 ppm at reaction temperature of 250°C; reduction peak temperature of 280 vs. 315°C. Study of the reducibility of CuO-ZnO catalysts by Fierro et al.[49] using H_2-TPR demonstrated that the synergistic effect presented at the interface between CuO and ZnO minicrystals in the Cu/ZnO catalysts and would be improved with enhanced surface contact between CuO and ZnO minicrystals. This practically promoting the reducibility of CuO in the catalysts (*i.e.*, reduction peak temperature is significantly decreased). Accordingly, it is believed that the CuZnAl-A-600 catalyst derived from HTLcs synthesized using Cu/Zn acetates provided stronger interaction between CuO and ZnO minicrystal (thereby leading to enhanced synergistic effect) than the CuZnAl-N-600 catalyst derived from HTLcs synthesized using Cu/Zn nitrates.

Fierro et al.[49] also pointed out that the initial dispersion of CuO and its interaction with ZnO certainly affect the ability of re-oxidation of metallic copper in the reduced CuO-ZnO catalysts with CO_2. The copper strongly interacted with ZnO that showed promoted reducibility is reactive to be re-oxidized by CO_2. Accordingly, the fraction of CO_2-oxidizable copper for CuZnAl-A-600 and CuZnAl-N-600 catalysts was measured using H_2-CO_2-H_2 red/ox cycle, wherein the CO_2 oxidation was performed at 300°C for 1 h prior to the second regular H_2-TPR test. Not surprisingly, the former catalyst afforded a CO_2-reoxidized copper fraction of 9.2%, being higher than the value of 7.8% for the latter one. This further confirms the conclusion that interaction between CuO and ZnO minicrystal in the CuZnAl-A-600 catalyst is stronger than that in the CuZnAl-N-600 catalyst.

SEM photographes and EDX elemental mapping images of Cu and Zn for the CuZnAl-A-600 and CuZnAl-N-600 catalysts after reduction with H_2 at 300°C for 2 h are displayed in Supporting Information Figures 1 and 2. As we can see, the low-resolution morphology for both of them looks similar in Supporting Information Figure 1A1 and B1, but their high-resolution morphology is different in Supporting Information Figure 1A2 and B2. Flake-like morphology was observed for the CnZnAl-N-600 catalyst but amorphous-powder-like morphology for the CuZnAl-A-600 catalyst in their high-resolution images (Supporting Information Figure 1A2 and B2). The EDX elemental images show that copper and zinc dispersed more homogeneously for the CuZnAl-A-600 catalyst compared with the CuZnAl-N-600 catalyst (Supporting Information Figure 2). As a result, larger contact area between Cu and ZnO can be obtained thereby leading to obvious promotion on both the reducibility of CuO and the re-oxidation of Cu with CO_2.[49]

Furthermore, according to the previous study by Frost,[41] such copper placed in contact with the zinc oxide facilitates the formation of oxygen vacancies over catalyst surface due to the reduction of ionization energy, which made the activation of H_2O molecules significantly promoted to produce more surface active oxygen species. As a result, such enhanced concentration of surface active oxygen species improved the decomposition of the methyl formate intermediates to form formic acid[50,51] that would directly decompose to form CO_2 and H_2.[43,44] Therefore, direct decomposition of methyl formate intermediates would be significantly suppressed to form methanol and CO.[48]

At this point, it is reasonable to infer that the Cu-ZnO interaction in the catalysts governed selectivity to CO for the MSR process. The excellent selectivity to CO (*i.e.*, low CO concentration in reformate) for the CuZnAl-A-600 catalyst derived from HTLcs synthesized using acetates could be reasonably correlated to the stronger interaction between CuO and ZnO minicrystal (Supporting Information Figure 1) and increased Cu-ZnO interface area (Supporting Information Figure 2).

Conclusions

In summary, the optimized decomposition of CuZnAl HTLcs at 600°C, involving complete decomposition of the transitional $(Cu,Zn)Al_xO_y(CO_3)_z$ compounds provided an efficient way to produce highly active and stable CuZnAl MSR catalysts with enhanced copper dispersion and improved copper reducibility compared with those decomposed at or over 700°C and at or below 500°C. The most special advantage of this decomposition behavior is to produce highly dispersed CuO particles accompanied by the formation of $CuAl_2O_4$ spinel phase that played a key role in separating and stabilizing the nanosized Cu and ZnO during the reaction. Moreover, the prereduction treatment between startup and shutoff can be omitted, which is an important reformer consideration for application in portable or mobile fuel cell power system.

Most interestingly, the change of Cu/Zn starting metal materials made remarkable difference in performance of the resulting MSR catalysts. The MSR performance of the HTLcs-derived CuZnAl catalysts ranked as following orders: acetates $\sim$ nitrates $\gg$ chlorides $\sim$ sulfates for the reactivity; acetates $<$ nitrates $\ll$ chlorides $\sim$ sulfates for the selectivity to CO. CuZnAl-A-600 afforded much lower CO

concentration in the dry product gas compared with the CuZnAl-N-600 prepared from nitrates: 0.04–0.05% (400–500 ppm) vs. ~0.2% (2000 ppm) with >95% methanol conversion under compatible reaction conditions (250°C and a WHSV of 2.5 h^{-1}). Over the CuZnAl-A-600, CO of ~0.005% (~50 ppm) in the dry product gas could be obtained with near complete methanol conversion at 210°C with a small WHSV of 0.5 h^{-1} and remained in entire 100-h test. It is safe to say that one-step generation of H_2, with the CO concentration as low as the requirement (<100 ppm or 0.01%) in PEMFC application, is possible *via* MSR process over the rationally designed CuZnAl catalysts.

By combining the reaction results with the information provided by various characterizations such as H_2-TPR, H_2-CO_2-H_2 red/ox cycle, CO_2-TPD and SEM/EDX analyses, it is believed that the CuZnAl-A-600 catalyst derived from HTLcs synthesized using Cu/Zn acetates permitted stronger interaction between CuO and ZnO minicrystal and larger Cu-ZnO contact interface thereby leading to significant reduction of CO formation during the MSR process. This is probably due to the significant improvement of hydrolysis of the methyl formate intermediates to form formic acid and the extreme suppression of their direct decomposition form methanol and CO.

Acknowledgments

Y. Lu gratefully thanks the Program for New Century Excellent Talents in University (NCET-06-0423), Shuguang Project (06SG28) and Shanghai Leading Academic Discipline Project (B409). This work is supported by the National Natural Science Foundation of China (20590366, 20573036), the Ministry of Science and Technology of China (2007AA05Z101) and the Science & Technology Commission of Shanghai Municipality (06SR07101).

Literature Cited

1. Hamelinck CN, Faaij APC. Future prospects for production of methanol and hydrogen from biomass. *J Power Sources*. 2002; 111:1–22.
2. Lindström B, Pettersson LJ. Development of a methanol fuelled reformer for fuel cell applications. *J Power Sources*. 2003;118:71–78.
3. Wang L-C, Liu Y-M, Chen M, Cao Y, He H-Y, Wu G-S, Dai W-L, Fan K-N. Production of hydrogen by steam reforming of methanol over Cu/ZnO catalysts prepared via a practical soft reactive grinding route based on dry oxalate-precursor synthesis. *J Catal*. 2007;246: 193–204.
4. Shishido T, Yamamoto Y, Morioka H, Takaki K, Takehira K. Active Cu/ZnO and Cu/ZnO/Al_2O_3 catalysts prepared by homogeneous precipitation method in steam reforming of methanol. *Appl Catal A*. 2004;263:249–253.
5. Agarwal V, Patel S, Pant KK. H_2 production by steam reforming of methanol over Cu/ZnO/Al_2O_3 catalysts: transient deactivation kinetics modeling. *Appl Catal A*. 2005;279:155–164.
6. Huang CY, Sun YM, Chou CY, Su CC. Performance of catalysts CuO-ZnO-Al_2O_3, CuO-ZnO-Al_2O_3-Pt-Rh, and Pt-Rh in a small reformer for hydrogen generation. *J Power Sources*. 2007;166:450–457.
7. Ma L, Gong B, Tran T, Wainwright MS. Cr_2O_3 promoted skeletal Cu catalysts for the reactions of methanol steam reforming and water gas shift. *Catal Today*. 2000;63:499–505.
8. Zhang X-R, Wang L-C, Yao CZ, Cao Y, Dai W-L, He H-Y, Fan KN. Preparation of a highly efficient Cu/ZnO/Al_2O_3 catalyst via gel-coprecipitation of oxalate precursors for low-temperature steam reforming of methanol. *Catal Lett*. 2005;102:183–190.
9. Patel S, Pant KK. Activity and stability enhancement of copper-alumina catalysts using cerium and zinc promoters for the selective production of hydrogen via steam reforming of methanol. *J Power Sources*. 2006;159:139–143.
10. Jeong H, Kim KI, Kim TH, Ko CH, Park HC, Song IK. Hydrogen production by steam reforming of methanol in a micro-channel reactor coated with Cu/ZnO/ZrO_2/Al_2O_3 catalyst. *J Power Sources*. 2006;159:1296–1299.
11. Dubey A, Kannan S. Liquid phase hydroxylation of benzene over Cu-containing ternary hydrotalcites. *Catal Commun*. 2005;6:394–398.
12. Turco M, Bagnasco G, Costanition U, Marmottini F, Montanari T, Ramis G, Busca G. Production of hydrogen from oxidative steam reforming of methanol. I. Preparation and characterization of Cu/ZnO/Al_2O_3 catalysts from a hydrotalcite-like LDH precursor. *J Catal*. 2004;228:43–55.
13. Turco M, Bagnasco G, Costanition U, Marmottini F, Montanari T, Ramis G, Busca G. Production of hydrogen from oxidative steam reforming of methanol. II. Catalytic activity and reaction mechanism on Cu/ZnO/Al_2O_3 hydrotalcite-derived catalysts. *J Catal*. 2004;228: 56–65.
14. Kniep BL, Girgsdies F, Ressler T. Effect of precipitate aging on the microstructural characteristics of Cu/ZnO catalysts for methanol steam reforming. *J Catal*. 2005;236:34–44.
15. Schur M, Bems B, Dassenoy A, Kassatkine I, Urban J, Wilmes H, Hinrichsen O, Muhler M, Schlögl R. Continuous coprecipitation of catalysts in a micromixer: Nanostructured Cu/ZnO composite for the synthesis of methanol. *Angew Chem Int Ed*. 2003;42:3815–3817.
16. Günter MM, Ressler T, Hentoft RE, Bems B. Redox behavior of copper oxide/zinc oxide catalysts in the steam reforming of methanol studied by in situ x-ray diffraction and absorption spectroscopy. *J Catal*. 2001;203:133–149.
17. Taylor SH, Hutchings GJ, Mirzaei AA. Copper zinc oxide catalysts for ambient temperature carbon monoxide oxidation. *Chem Commun*. 1999;1373–1374.
18. Kniep BL, Ressler T, Rabis A, Girgsdies F, Baenitz M, Steglich F, Schlögl R. Rational design of nanostructured copper-zinc oxide catalysts for the steam reforming of methanol. *Angew Chem Int Ed*. 2004;43:112–115.
19. Ressler T, Kniep BL, Kasatkin I, Schlögl R. The microstructure of copper zinc oxide catalysts: bridging the materials gap. *Angew Chem Int Ed*. 2005;44:4704–4707.
20. Shen JP, Song C. Influence of preparation method on performance of Cu/Zn-based catalysts for low-temperature steam reforming and oxidative steam reforming of methanol for H2 production for fuel cells. *Catal Today*. 2002;77:89–98.
21. Murcia-Mascarós S, Navarro RM, Gómez-Sainero L, Costantino U, Nocchetti M, Fierro JLG. Oxidative methanol reforming reactions on cuznal catalysts derived from hydrotalcite-like precursors. *J Catal*. 2001;198:338–347.
22. Velu S, Suzuki K, Okazaki M, Kappor MP, Osaki T, Ohashi F. Oxidative steam reforming of methanol over cuznal(zr)-oxide catalysts for the selective production of hydrogen for fuel cells: catalyst characterization and performance evaluation. *J Catal*. 2000;194:373–384.
23. Narayanan S, Krishna K. Structure activity relationship in Pd/hydrotalcite: effect of calcination of hydrotalcite on palladium dispersion and phenol hydrogenation. *Catal Today*. 1999;49:57–63.
24. Kannan S, Rives V, Knozinger H. High-temperature transformations of Cu-rich hydrotalcites. *J Solid State Chem*. 2004;177:319–331.
25. Lu Y, Wang Y, Gao LD, Chen JC, Mao JP, Xue QS, Liu Y, Wu HH, Gao GH, He M-Y. Aerobic oxidative desulfurization: a promising new approach for sulfur removal from fuels. *ChemSusChem*. 2008;1:302–306.
26. Lu Y, Chen JC, Liu Y, Xue QS, He M-Y. Highly sulfur-tolerant Pt/$Ce_{0.8}Gd_{0.2}O_{1.9}$ catalyst for steam reforming of liquid hydrocarbons in fuel cell applications. *J. Catal*. 2008;254:39–48.
27. Bond GC, Namijo SN. An improved procedure for estimating the metal surface area of supported copper catalysts. *J Catal*. 1989; 118:507–510.
28. Santacesaria E, Carra S. Kinetics of catalytic steam reforming of methanol in a CSTR reactor. *Appl Catal*. 1983;5:345–358.
29. Kanaii Y, Watanabe T, Fujitani T, Uchijima T, Nakamura J. The synergy between Cu and ZnO in methanol synthesis catalysts. *Catal Lett*. 1996;38:157–163.
30. Melian-Cabrera I, Granados ML, Fierro JLG. Thermal decomposition of a hydrotalcite- containing Cu-Zn-Al precursor: thermal methods combined with an in situ DRIFT study. *Phys Chem Chem Phys*. 2002;4:3122–3127.

31. Idem RO, Bakhshi NN. Production of hydrogen from methanol. II. Experimental studies. *Ind Eng Chem Res*. 1994;33:2056–2065.
32. Breen JP, Meunier FC, Ross JRH. Mechanistic aspects of the steam reforming of methanol over a $CuO/ZnO/ZrO_2/Al_2O_3$ catalyst. *Chem Commun*. 1999;2247–2248.
33. Idem RO, Bakhshi NN. Kinetic modeling of the production of hydrogen from the methanol-steam reforming process over Mn-promoted coprecipitated Cu-Al catalyst. *Chem Eng Sci*. 1996;51:3697–3708.
34. Idem RO, Bakhshi NN. Production of hydrogen from methanol over promoted coprecipitated cu-al catalysts: the effects of various promoters and catalyst activation methods. *Ind Eng Chem Res*. 1995;34:1548–1557.
35. Prerez-Ramirez J, Mul G, Moulijn JA. In situ Fourier transform infrared and laser Raman spectroscopic study of the thermal decomposition of Co-Al and Ni-Al hydrotalcites. *Vib Spectrosc*. 2001; 27:75–88.
36. Yang RQ, Fu YL, Zhang Y, Tsubaki N, In situ DRIFT study of low-temperature methanol synthesis mechanism on Cu/ZnO catalysts from CO_2-containing syngas using ethanol promoter. *J Catal*. 2004;228:23–35.
37. López T, Bosch P, Asomoza M, Gómez R, Ramos E. DTA-TGA and FTIR spectroscopies of sol-gel hydrotalcites: aluminum source effect on physicochemical properties. *Mater Lett*. 1997;31:311–316.
38. Barton J, Pour V. Kinetics of catalytic conversion of methanol at higher pressures. *Collect Czech Chem Commun*. 1980;45:3402–3407.
39. Chen HY, Lau SP, Chen L, Lin J, Huan CHA, Tan KL, Pan JS. Synergism between Cu and Zn sites in Cu/Zn catalysts for methanol synthesis. *Appl Surf Sci*. 1999;152:193–199.
40. Klier K. Methanol synthesis. *Adv Catal*. 1982;31:243–313.
41. Frost JC. Junction effect interactions in methanol synthesis catalysts. *Nature*. 1988;334:577–580.
42. Neophytides SG, Marchi AJ, Froment GF. Methanol synthesis by means of diffuse reflectance infrared Fourier transform and temperature-programmed reaction spectroscopy. *Appl Catal A*. 1992;86:45–64.
43. Takahashi K, Takezawa N, Kobayashi H. The mechanism of steam reforming of methanol over a copper-silica catalyst. *Appl Catal*. 1982;2:363–366.
44. Takezawa N, Iwasa N. Steam reforming and dehydrogenation of methanol: Difference in the catalytic functions of copper and group VIII metals. *Catal Today*. 1997;36:45–56.
45. Breen JP, Ross JRH. Methanol reforming for fuel-cell applications: development of zirconia-containing Cu-Zn-Al catalysts. *Catal Today*. 1999;51:521–533.
46. Jiang CJ, Trimm DL, Wainwright MS, Cant NW. Kinetic mechanism for the reaction between methanol and water over a copper-zinc oxide-alumina catalyst. *Appl Catal A*. 1993;97:145–158.
47. Peppley BA, Amphlett JC, Kearns LM, Mann RF. Methanol-steam reforming on $Cu/ZnO/Al_2O_3$ catalysts. Part 2: A comprehensive kinetic model. *Appl Catal A*. 1999;179:31–49.
48. Higdon BW, Hobbs CC, Onore MJ. 1974 US Patent 3,812,210.
49. Fierro G, Jacono ML, Inversi M, Porta P, Cioci F, Lavecchia R. Study of the reducibility of copper in CuO-ZnO catalysts by temperature-programmed reduction. *Appl Catal A*. 1996;137:327–348.
50. Zhang R, Sun Y-H, Peng S-Y. In situ FTIR studies of methanol adsorption and dehydrogenation over Cu/SiO_2 catalyst. *Fuel*. 2002;81:1619–1624.
51. Millar GJ, Rochester CH, Waugh KC. Infrared study of the adsorption of methanol on oxidized and reduced copper/silica catalysts. *J Chem Soc Faraday Trans*. 1991;87:2795–2804.

Manuscript received Feb. 26, 2008, and revision received Oct. 10, 2008.